J. Microbiol. Biotechnol. (2011), **21**(1), 5–13
doi: 10.4014/jmb.1008.08018
First published online 19 November 2010

JOURNAL OF MICROBIOLOGY AND BIOTECHNOLOGY

Chemotaxonomy of *Trichoderma* spp. Using Mass Spectrometry-Based Metabolite Profiling

Kang, Daejung[1], Jiyoung Kim[1], Jung Nam Choi[1], Kwang-Hyeon Liu[2], and Choong Hwan Lee[1]*

[1]*Department of Bioscience and Biotechnology, Kon-Kuk University, Seoul 143-701, Korea*
[2]*Department of Pharmacology and PharmacoGenomics Research Center, Inje University College of Medicine, Busan 614-735, Korea*

Received: August 17, 2010 / Revised: September 20, 2010 / Accepted: September 28, 2010

In this study, seven *Trichoderma* species (33 strains) were classified using secondary metabolite profile-based chemotaxonomy. Secondary metabolites were analyzed by liquid chromatography–electrospray ionization tandem mass spectrometry (LC–ESI–MS–MS) and multivariate statistical methods. *T. longibrachiatum* and *T. virens* were independently clustered based on both internal transcribed spacer (ITS) sequence and secondary metabolite analyses. *T. harzianum* formed three subclusters in the ITS-based phylogenetic tree and two subclusters in the metabolite-based dendrogram. In contrast, *T. koningii* and *T. atroviride* strains were mixed in one cluster in the phylogenetic tree, whereas *T. koningii* was grouped in a different subcluster from *T. atroviride* and *T. hamatum* in the chemotaxonomic tree. Partial least-squares discriminant analysis (PLS-DA) was applied to determine which metabolites were responsible for the clustering patterns observed for the different *Trichoderma* strains. The metabolites were hetelidic acid, sorbicillinol, trichodermanone C, giocladic acid, bisorbicillinol, and three unidentified compounds in the comparison of *T. virens* and *T. longibrachiatum*; harzianic acid, demethylharzianic acid, homoharzianic acid, and three unidentified compounds in *T. harzianum* I and II; and koninginin B, E, and D, and six unidentified compounds in *T. koningii* and *T. atroviride*. The results of this study demonstrate that secondary metabolite profiling-based chemotaxonomy has distinct advantages relative to ITS-based classification, since it identified new *Trichoderma* clusters that were not found using the latter approach.

Keywords: *Trichoderma*, chemotaxonomy, liquid chromatography–mass spectrometry, multivariate analysis, metabolomics

**Corresponding author*
Phone: +82-2-2049-6177; Fax: +82-2-455-4291;
E-mail: chlee123@konkuk.ac.kr

Members of *Trichoderma* are the most common saprophytic fungi and are found in almost all agriculture soils worldwide. The genus was identified 200 years ago by Persoon (1794), and approximately 130 species have been classified [4]. Certain species of *Trichoderma* have been known to produce important secondary metabolites such as antibiotics, plant growth regulators, and mycotoxins, which are mainly used to protect plants from pathogens [21, 22, 26]. In fact, *T. harzianum* and *T. atroviride* are commercially used as biocontrol agents [27]. The compounds produced by some *Trichoderma* species are harmful to animals. Thus, it is necessary to identify and classify *Trichoderma* fungi based on their metabolites and to determine which properties and characteristics of a species are associated with particular compounds. The identification and classification of *Trichoderma* species usually rely on morphology and utilization of nutrients; however, it is difficult to distinguish between two closely related species using these approaches. Although DNA sequences can also be used to separate fungi at the species level, approximately 40% of the database sequences of *Trichoderma* species have either been misidentified or remain unidentified at the species level [6, 14]. As an alternative method, chemotaxonomy may allow one to utilize secondary metabolites to distinguish fungi at the species level [8]. Several studies on the chemotaxonomy of *Trichoderma* have been reported [21, 25]; however, these studies did not identify the metabolites that determined different clustering patterns. Metabolite profiling is often used to identify unknown compounds from complex data because it makes possible the simultaneous observation of all kinds of metabolites. Liquid chromatography–mass spectrometry (LC–MS) is popularly applied to the specific detection of unknown metabolites in complex chemical or biological samples owing to its specificity and high sensitivity [12, 20]. In particular, metabolomic approaches that include multivariate statistical analyses such as principal component analysis

(PCA) and partial least-squares discriminant analysis (PLS-DA) are high-throughput methods of determining significantly different metabolites by LC–MS. Therefore, LC–MS is a suitable and powerful tool for the classification of microorganisms based on metabolite profiling [12]. In the present study, *Trichoderma* species were classified based on their secondary metabolite profiles using LC–MS–MS.

Materials and Methods

Chemicals and Reagents

HPLC-grade water, methanol, and acetonitrile were purchased from Burdick and Jackson (Muskegon, MI, USA). Malt extract agar (MEA) was purchased from Becton Dickinson (Franklin Lakes, NJ, USA). Analytical-grade formic acid, pyridine, methoxyamine hydrochloride, and *N*-methyl-*N*-(trimethylsilyl) trifluoroacetamide (MSTFA) were purchased from Sigma Aldrich (St. Louis, MO, USA).

Fungal Strains and Culture Conditions

The *Trichoderma* strains used in this study are listed in Table 1. All of the strains were obtained from the Korean Agricultural Culture Collection (KACC; Republic of Korea). The cultures were grown on MEA plates for 7 days at 28°C in the dark and then the spores were harvested and stored in 20% glycerol at −70°C. *Trichoderma* was cultured on MEA plates for 3 days and three young mycelia pieces (6-mm diameter) were placed on fresh MEA plates. To determine the cultivation time, four agar pieces were periodically harvested from 0 to 18 days at 2-day intervals and extracted with ethyl acetate. The fungal extracts were analyzed by LC–MS and a statistical method was used to identify the optimal cultivation time for the chemotaxonomy studies.

Extraction of Fungal Metabolites

Fungal disks (6-mm diameter) were collected from four different places: the center of the colony, between the center and the rim of the colony, the rim of the colony farthest from other colonies, and the rim of the colony closest to adjacent colonies [23]. The agar pieces were transferred to 3 ml of ethyl acetate and mixed on a rotary shaker at 200 rpm for 9 h, and the solvent was evaporated using a speed vacuum [18]. The concentrated extracts were dissolved in 100 µl of methanol, passed through a 0.45-µm disposable PTFE filter, and used for LC–MS analysis.

LC–ESI–MS–MS Analysis of *Trichoderma* Metabolites

Liquid chromatographic analysis was performed on a Varian 500MS ion trap mass spectrometer (Varian, Inc., Palo Alto, CA, USA), which consisted of an LC pump (Varian 212), a photodiode array detector (ProStar 335), and an autosampler (ProStar 410). The LC system was equipped with a 100×2.0 mm C18 column with a 3-µm particle size (Varian). The binary mobile phase consisted of water and acetonitrile with 0.1% (v/v) formic acid. The initial gradient of the mobile phase was 10% acetonitrile for 2 min, and was gradually increased to 100% acetonitrile over 28 min. It was maintained at 100% acetonitrile for 5 min, and then sharply reduced to 10% acetonitrile for 0.06 min and maintained for 5 min. Ten µl of each sample was injected and the flow rate was maintained at 0.2 ml/min.

Table 1. Taxa of *Trichoderma* determined by *Trich*OKEY.

KACC No.[a]	Taxon	Accession No.[b]	*Trich*OKEY[c]
40764	*T. harzianum*	KA000708	*T. harzianum*
40792	*T. harzianum*	KA000249	*T. harzianum*
40785	*T. harzianum*	KA000242	*T. harzianum*
40789	*T. harzianum*	KA000246	*T. harzianum*
40790	*T. harzianum*	KA000247	*T. harzianum*
40795	*T. harzianum*	KA000252	*T. harzianum*
40796	*T. harzianum*	KA000253	Unknown
40883	*T. harzianum*	KA000258	*T. pleuroticola*
40884	*T. harzianum*	KA000263	*T. harzianum*
40885	*T. harzianum*	KA000264	*T. harzianum*
40875	*T. aggressivum*	KA000915	*T. aggressivum*
40874	*T. aggressivum*	KA000193	*T. aggressivum*
40876	*T. aggressivum*	KA000194	*T. aggressivum*
40866	*T. virens*	KA000703	*T. virens*
41754	*T. virens*	KA000705	*T. virens*
40929	*T. virens*	KA000261	*T. virens*
40800	*T. virens*	KA000257	*T. virens*
40867	*T. virens*	KA000704	*T. virens*
40798	*T. longibrachiatum*	KA000255	*T. longibrachiatum*
40887	*T. longibrachiatum*	KA000260	*T. longibrachiatum*
40540	*T. longibrachiatum*	KA000674	*T. longibrachiatum*
40563	*T. longibrachiatum*	KA000675	*T. longibrachiatum*
40799	*T. longibrachiatum*	KA000256	*T. longibrachiatum*
40769	*T. hamatum*	KA000659	*T. hamatum*
40869	*T. hamatum*	KA000759	*T. hamatum*
40779	*T. koningii*	KA000237	*T. koningii*
40878	*T. koningii*	KA000672	*T. koningii*
40548	*T. koningii*	KA000762	*T. atroviride*
40775	*T. atroviride*	KA000005	*T. atroviride*
42248	*T. atroviride*	KA001623	*T. atroviride*
40868	*T. atroviride*	KA000649	*T. atroviride*
40776	*T. atroviride*	KA000006	Unknown
40774	*T. atroviride*	KA000004	*T. atroviride*

[a]KACC, Korean Agricultural Culture Collection.
[b]ITS1, ITS2, and 5.8S sequences of ribosomal DNA obtained from the KACC Web site (http://kacc.rda.go.kr).
[c]Oligonucleotide barcode tool for the identification of *Trichoderma* sp. (http://www.isth.info).

ESI–MS was performed in negative mode within a range of *m/z* 100–1,000. The running parameters were as follows: drying temperature, 350°C; needle voltage, 5 kV; capillary voltage, 70 V; drying gas pressure (nitrogen), 10 psi; and nebulizer gas pressure (air), 35 psi. MS^n analysis was performed using scan-type turbo data-dependent scanning (DDS) under the same conditions used for negative-mode MS scanning.

GC-MS Analysis of *Trichoderma*

Gas chromatography–mass spectrometry (GC–MS) data were compared with the LC–MS data to select the appropriate technique for determining *Trichoderma* chemotaxomy. The GC–MS analyses were performed on a Varian 4000 electron impact mass spectrometer using a Varian CP-8400 injector. A 30 m×0.25 mm FactorFour

capillary column with a particle size of 0.25 μm (Varian) was used. The injection temperature was set at 250°C. The helium gas flow rate through the column was 1 ml/min, ions were generated at an electron impact (EI) of 70 kV, the ion source temperature was set at 200°C, and the mass range was *m/z* 50–1,000. The column temperature was maintained isothermally at 70°C for 2 min and then raised to 300°C at a rate of 10°C/min. For derivatization, all of the samples were dissolved in 30 μl of methoxyamine hydrochloride in pyridine (20 mg/ml) for the first derivatization and incubated at 75°C for 30 min. MSTFA (30 μl) was added and incubated at 75°C for 30 min as the second derivatization.

UPLC–Q-TOF-MS Analysis

Ultra performance liquid chromatography–quadrupole time-of-flight (UPLC–Q-TOF) mass spectrometry was performed using a Waters Micromass Q-TOF Premier with UPLC Acquity System (Waters, Milford, MA, USA) to measure accurately the molecular weight of the metabolites. This system contained a 100×2.1 mm Acquity UPLC BEH C18 column (Waters) with a particle size of 1.7 μm. The mobile phase consisted of water and acetonitrile with 0.1% formic acid (v/v). The initial gradient of the mobile phase was maintained at 0% acetonitrile for 0.3 min, gradually increased to 30% acetonitrile over 3 min, increased to 40% acetonitrile for 1 min, and then gradually increased to 100% acetonitrile for 8 min. It was maintained at 100% acetonitrile for 2 min, and then 0% acetonitrile was maintained for 2 min. Five μl of the sample was injected and the flow rate was maintained at 0.3 ml/min. ESI was performed in the negative and positive modes within a range of *m/z* 100–1,000. The operating parameters were as follows: ion source temperature, 200°C; cone gas flow, 50 l/h; desolvation gas flow, 600 l/h; capillary voltage, 2.8 kV; and cone voltage, up to 35 V.

Data Processing

LC–MS data were analyzed using Varian MS Workstation 6.9 software. The LC–ESI–MS negative-mode chromatogram raw data files were converted into the network common data form (netCDF, *.cdf) by Vx Capture 2.1 software (Adron Systems LLC, Laporte, MN, USA). The netCDF files were automatically aligned and compared with the mass spectrometry datasets by the MetAlign software package (http://www.metalign.nl) [15]. The MetAlign parameters were set at a peak slope factor of 1.0, peak threshold factor of 2.0, peak threshold of 15, and average peak width at half height of 7.0, which corresponds to a retention time of 2–35 min and mass range of 100–1,000 for LC–MS. A peak threshold of 5.0 and average peak width at half height of 3.0 were used in the case of GC–MS. The *.csv file output contained the nominal mass peak intensity data with retention time and was transferred to an Excel datasheet for multivariate analysis.

Statistical Analysis

Multivariate statistical analysis was performed using SIMCA-P+ 12.0 (Umetrics, Umea, Sweden). Log_{10}-transformed MS data were mean-centered with unit variance scaling for statistical analysis. The unsupervised principal component analysis (PCA) was used to observe the distribution of *Trichoderma* strains. The largest variance was separated in the first principal component (PC1), and the second principal component (PC2) was orthogonal to PC1. Hierarchical clustering analysis (HCA) reasonably divided *Trichoderma* strain groups according to homologous metabolite profiling. Two groups from HCA were separated by supervised PLS-DA and their potential variables were selected based on variable importance in the projection (VIP>2.0) values and *p*-value ($p<0.001$). The *p*-value between different metabolite-based cluster groups was determined using Stastistica 7 (StatSoft, Inc., Tulsa, OK, USA). The significantly different secondary metabolites were confirmed in the LC–MS chromatogram. The metabolites were tentatively identified by molecular weight, retention time, UV spectra, MS^n fragmentation pattern analysis, and high-resolution mass data (Q-TOF-MS) using the *Dictionary of Natural Products* (Copyright 2008, Taylor & Francis Group, Boca Raton, FL, USA), Antibase 3.0 (CambridgeSoft Corporation, Cambridge, MA, USA), and published literature. The MS^n fragmentation pattern of each metabolite was compared with the simulated character of fragmentation using Mass Frontier Software 4.0 (HighChem, Bratislava, Slovakia) [12].

Genetic Information

The internal transcribed spacer 1 (ITS1), 5.8 S gene, and ITS2 sequences of the ribosomal DNA of *Trichoderma* species were collected from the KACC (http://kacc.rda.go.kr) (Table 1). The sequences were aligned and analyzed by MEGA4 (Center for Evolutionary Functional Genomics, The Biodesign Institute, Tempe, AZ, USA) [24], and the phylogenetic tree was inferred using neighbor-joining algorithms with maximum composite likelihood. The stability of clusters was estimated with 1,000 bootstrap replications. Distances in the phylogenic tree represented differences in DNA sequences and expected evolutionary relationships. In addition, *Trich*OKEY 2 (ISTH Team, Vienna, Austria) was used to confirm the phylogenetic tree determined by ITS. The sequences were subjected to a parallel NCBI BLAST search to determine the best match or degree of similarity in order to identify *Trichoderma* species [5].

RESULTS

ITS-Based Phylogenetic Classification

A phylogenetic tree was established based on the ITS1, 5.8S, and ITS2 sequences of the ribosomal DNA of 7 species and 33 strains of *Trichoderma*. *Hypocrea aureoviridis* (CBS 245.63, Accession No. Z48819) was adjusted as an outgroup to branch the dendrogram more precisely (Fig. 1) [13]. The phylogenetic tree was divided into three main branches: *T. harzianum, T. aggressivum*, and *T. virens*; *T. longibrachiatum*; and *T. hamatum, T. atroviride*, and *T. koningii*. The *T. virens* group (bootstrap value, 98%) was clustered away from *T. harzianum* and *T. aggressivum*. The bootstrap value between *T. aggressivum* and *T. harzianum* spp. was no more than 55%, since the differences in base sequences were not remarkable. The *T. harzianum* strains were clustered in one group (bootstrap value, 71%), which was divided into three subclusters. Intraspecies variation in *T. harzianum* has already been reported [9, 13, 21]. *T. longibrachiatum*, *T. hamatum*, *T. atroviride*, and *T. koningii* were included in the second major branch. *T. hamatum* (bootstrap value, 100%) was discriminated from *T. koningii* and *T. atroviride*. *T.*

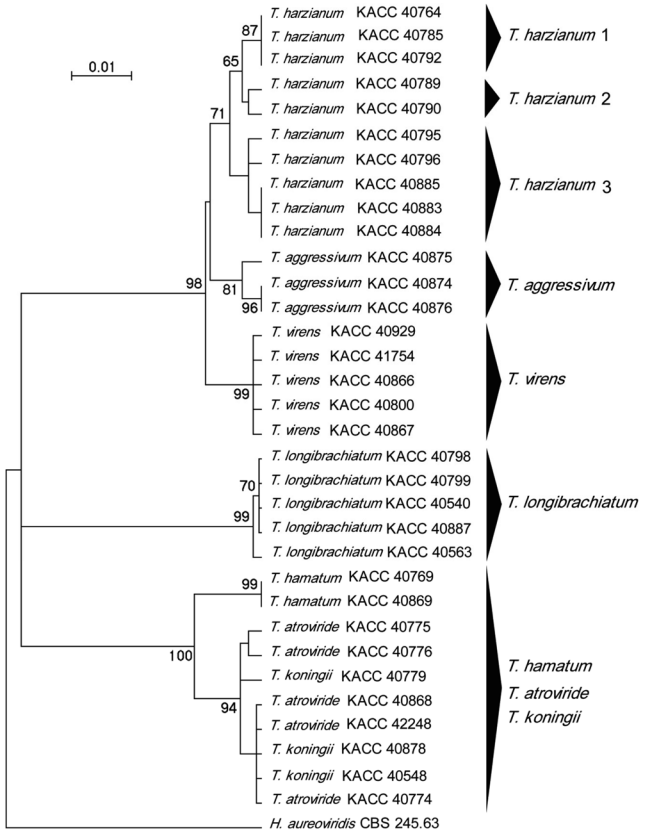

Fig. 1. Phylogenetic tree inferred from the neighbor-joining analysis of ITS1, 5.8S, and ITS2 sequences of ribosomal DNA. *H. aureoviridis* (CBS 245.63, Accession No. Z48819) was used as an outgroup. The numbers above the nodes represent bootstrap values from 1,000 bootstrap replications. The numbers given over branches indicate bootstrap coefficients >65%. Scale bar, 0.01 substitutions per nucleotide position.

koningii and *T. atroviride* were in the same cluster; the minor differences in the ITS between these two species, which caused them to be in the same group, have already been studied [16]. *Trich*OKEY 2 was used to compare the 33 *Trichoderma* strains based on ITS1, 5.8S, and ITS2 sequences. Twenty-nine strains were well-matched with the KACC categories; however, *T. harzianum* KACC 40883 and *T. koningii* KACC 40548 were mismatched and *T. harzianum* KACC 40796 and *T. atroviride* KACC 40776 were unknown (Table 1).

Metabolite-Based Chemotaxonomy

The metabolites of three *Trichoderma* species, *T. harzianum*, *T. longibrachiatum*, and *T. virens*, were analyzed by LC–MS, and the PCA score plots that represented fermentation time-dependent metabolite profiles showed three characteristic patterns. Based on PCA, the metabolites were shown to vary the most in 16-day-old agar cultures. Hence, metabolite profiles based on the PCA score plots for PC1 (15.0%) and PC2 (9.3%) were determined for the 33

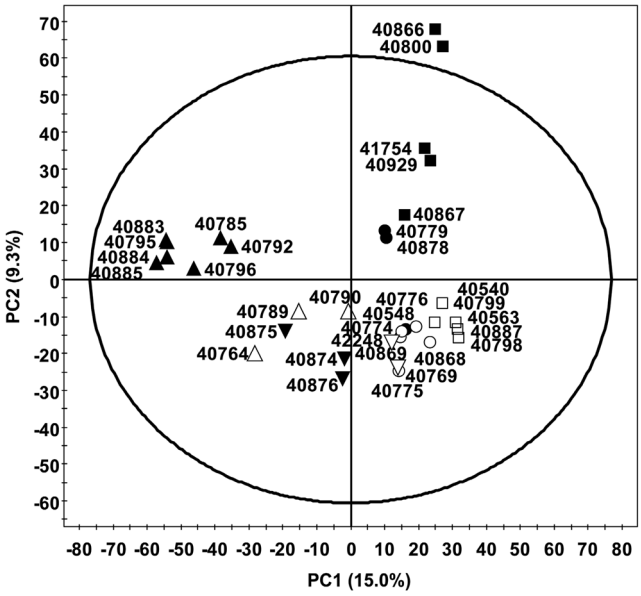

Fig. 2. Principle component analysis (PCA) score plots derived from the LC–MS dataset of *Trichoderma* spp. (▲ *T. harzianum* I, △ *T. harzianum* II, ▼ *T. aggressivum*, ■ *T. virens*, □ *T. longibrachiatum*, ▽ *T. hamatum*, ● *T. koningii*, and ○ *T. atroviride*).

strains of *Trichoderma* after 16 days of culture on agar (Fig. 2). PC1 to PC4 were used to reasonably divide the 33 strains of *Trichoderma* into clusters in the dendrogram based on the metabolite profiles (Fig. 3). Each group of *T. harzianum* I, *T. longibrachiatum*, and *T. virens* strains was clearly separated in the dendrogram. Three strains of *T. harzianum* II (KACC 40789, 40764, and 40790) were clustered with *T. aggressivum.* However, *T. atroviride, T. hamatum*, and *T. koningii* formed a mixed cluster; among them, *T. koningii* KACC 40779 and 40878 were grouped in a subcluster of the heterologous cluster. These interdifferences between clusters may reflect variations in metabolites.

GC–MS analysis was conducted using the same process of multivariate analysis and compared with the LC–MS results (Fig. S1). Components PC1 to PC10 were used to establish the dendrogram and cluster the strains. The GC–MS-based dendrogram produced various groups, which showed less correlation with the ITS-based classification of *Trichoderma* than did the LC–MS analysis. Thus, LC–MS-based metabolite profiling was used to classify the *Trichoderma* strains systematically.

Comparison of Chemotaxonomic and Phylogenetic Trees

After comparison of the taxonomic correlations based on disparate criteria, the ITS and secondary metabolites, several differences among the taxa detected by each classification method were observed. *T. harzianum*, *T. longibrachiatum*, and *T. virens* were clearly clustered in

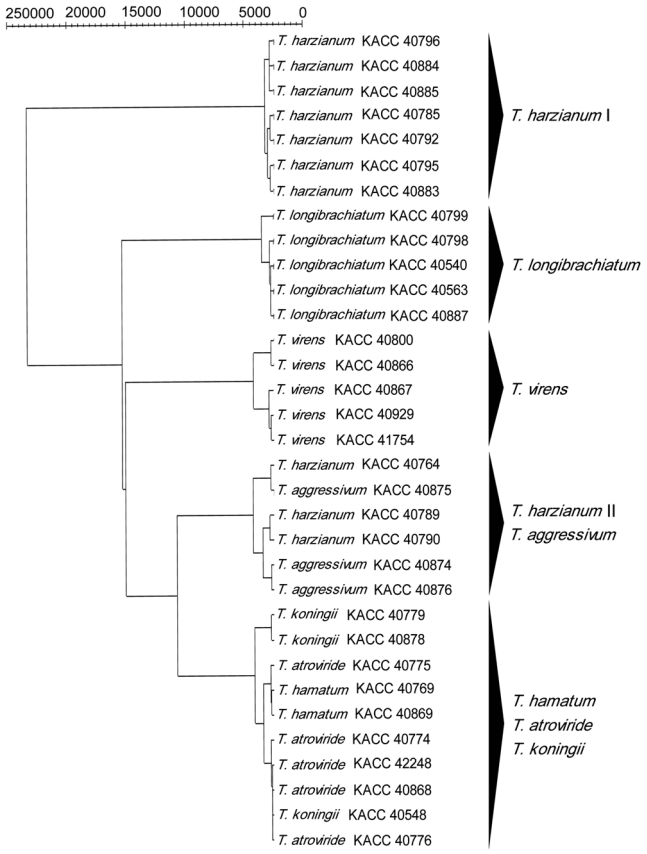

Fig. 3. LC–MS-based hierarchical clustering analysis (HCA) showing *Trichoderma* strain groups according to homologous metabolite profiling.

both the ITS-based phylogenetic tree and secondary metabolite-based chemotaxonomic tree. However, the *T. harzianum* strains were divided into three subclusters (*T. harzianum* 1, 2, and 3) in the ITS-based phylogenetic tree, whereas two distinct subclusters were observed in the chemotaxonomic tree, one being the unmixed *T. harzianum* I, and the other the heterologous subcluster containing *T. harzianum* II and *T. aggressivum. T. atroviride* and *T. koningii*, which belong to a section *Trichoderma*, have also been reported to share a very limited ITS variation [16]; they were clustered in an identical group in the ITS-based phylogenetic tree (Fig. 1). However, *T. koningii* formed an independent subcluster that was not mixed with other species in the chemotaxonomic dendrogram.

Identification of Significantly Classified Secondary Metabolites in Different Strains

The PLS-DA model was used to determine the variables that distinguished different strains. The secondary metabolite profiles of *T. virens* and *T. longibrachiatum* were analyzed by one orthogonal component with $R^2X=0.324$ and $Q^2=0.690$ (Fig. 4A). Potential variables to separate groups in the dendrogram were identified by loading plot with VIP> 2.0 and $p<0.001$ (Fig. 4B). Among the eight peaks used to characterize the species clusters, five compounds were tentatively identified as heptelidic acid, gliocladic acid, sorbicillinol, trichodermanone C, and bisorbicillinol. The significantly different metabolites derived from *T. virens* and *T. longibrachiatum* were significantly different in the box-and-whisker plot (Fig. 4C). Heptelidic acid and gliocladic acid have been known to be produced by *Gliocladium virens*, which is the commonly accepted synonym of *T. virens* [20]. In the *T. harzianum* I and *T. harzianum* II clusters, six distinguishing peaks were observed to be the main discriminating factors by PLS-DA with $R^2X=0.361$, $Q^2=0.532$ (Fig. 5A and 5B). Three peaks were identified as demethylharzianic acid, harzianic acid, and homoharzianic acid (Table 3). The intensity of hazianic acid and its derivatives was higher in *T. harzianum* I than II in the box-and-whisker plot (Fig. 5C). Harzianic acid is the main metabolite of *T. harzianum* in that the different groups of *T. harzianum* were worthy of note [28]. In the *T. koningii* and *T. atroviride* cluster, eight metabolites were analyzed by PLS-DA with $R^2X=0.439$, $Q^2=0.836$ (Fig. 6A and 6B; Table 4). Two of them were determined to be

Table 2. Significantly different metabolites between *T. longibrachiatum* and *T. virens.*

LC–ESI–MS–MS					UPLC–Q-TOF		
Tentative identification	t_R (min)	MW	$[M-H]^-$ MS^n fragment ions (*m/z*)	*p* Value (*t*-test)[a]	Measured $[M-H]^-$	Error (ppm)	Ref.
Heptelidic acid	10.4	280	279, 217, 174, 131	0.00E+00	279.1232	0	[10]
N.I.	10.9	298	297, 279, 253, 154	0.00E+00	297.1311	-	-
N.I.	11.5	266	265, 247, 205, 153	2.98E–04	265.1076	-	-
N.I.	12.5	282	281, 237, 193, 179	1.00E–06	281.1400	-	-
Sorbicillinol	12.8	248	247, 205, 192, 179	0.00E+00	247.0969	0.4	[2]
Gliocladic acid	13.1	254	253, 173, 157, 131	1.20E–05	253.1441	0.8	[10]
Trichodermanone C	13.5	394	393, 247, 205, 179	0.00E+00	293.1550	0.3	[17]
Bisorbicillinol	19.3	496	495, 433, 339, 247	3.60E–05	495.2016	0.4	[1]

t_R, Retention time; N.I., not identified.
[a]Indicated significant difference by *t*-test.

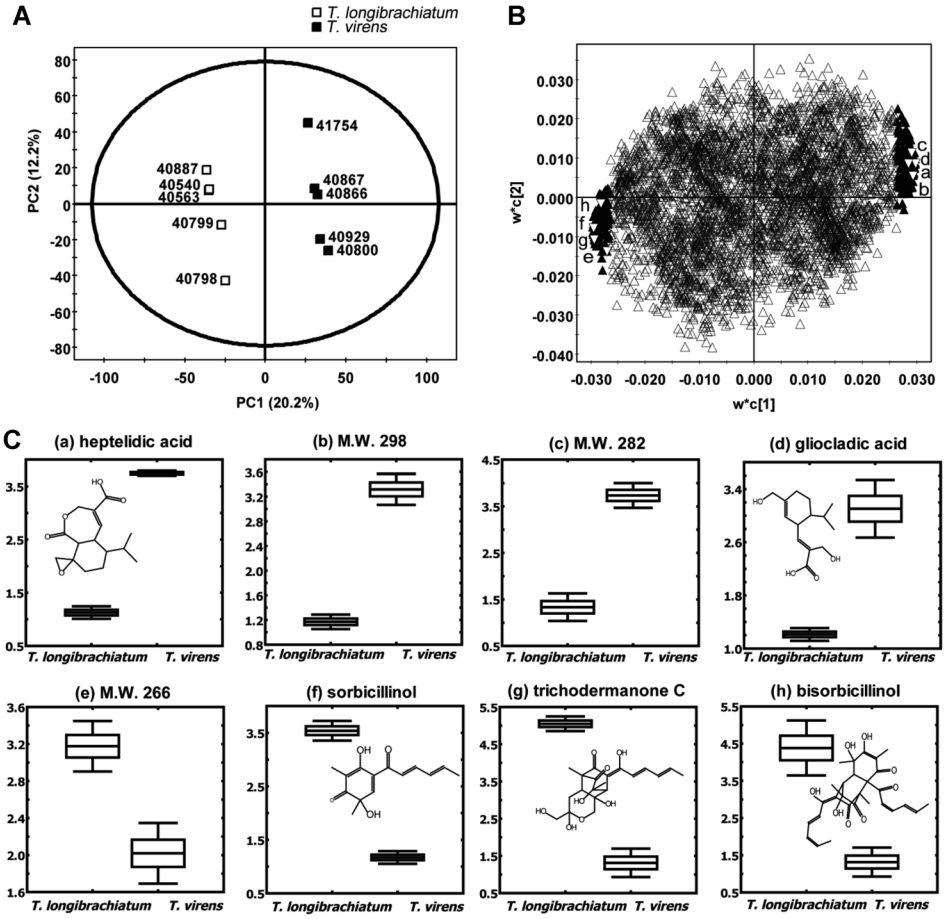

Fig. 4. PLS-DA score plots (**A**) and loading plots (**B**) of different clusters in the LC–MS-based dendrogram.
The selected variables (▲, VIP>2.0) and significantly different metabolites (▽) are highlighted in loading plots. Box-and-whisker plots showed significantly different secondary metabolites between *T. longibrachiatum* and *T. koningii* (**C**) (p<0.001). The Y axis of box-and-whisker plots indicates the LC–MS data transferred by $\log_{10}$.

koninginin B or E (previously reported to be stereoisomers [19]) and koninginin D, which were obtained as major metabolites in *T. koningii*, whereas the intensity of three of the six unidentified peaks was higher in *T. atroviride* (Fig. 6C). In Fig. S2, the LC–ESI–MS negative-ion chromatogram of *Trichoderma* sp. shows the positions of significantly different metabolites.

Discussion

It is difficult to classify *Trichoderma* species owing to insufficient morphologic and genetic variation; thus, misidentification often occurs [6, 14]. However, members of *Trichoderma* produce highly diverse metabolites that are species-specific; hence, polyphasic taxonomy using

Table 3. Significantly different metabolites between *T. harzianum* types I and II.

LC–ESI–MS–MS					UPLC–Q-TOF		
Tentative identification	t_R (min)	MW	$[M-H]^-$ MS^n fragment ions (*m/z*)	*p* Value (*t*-test)[a]	Measured $[M-H]^-$	Error (ppm)	Ref.
N.I.	15.8	465	464, 402, 382, 310	8.20E-05	464.2992	-	-
N.I.	16.9	201	200, 172, 156, 138	1.84E-04	200.0920	-	-
N.I.	17.4	408	407, 343, 309, 289	1.43E-03	407.2789	-	-
Harzianic acid	20.4	365	364, 346, 233, 180	3.63E-03	364.1755	1.1	[11]
Demethyharzianic acid	20.7	351	350, 332, 306, 192	2.03E-03	350.1605	0.6	[11]
Homoharzianic acid	23.5	379	378, 332, 233, 180	5.91E-04	378.1912	1.1	[11]

t_R, Retention time; N.I., not identified.
[a]Indicated significant difference by *t*-test.

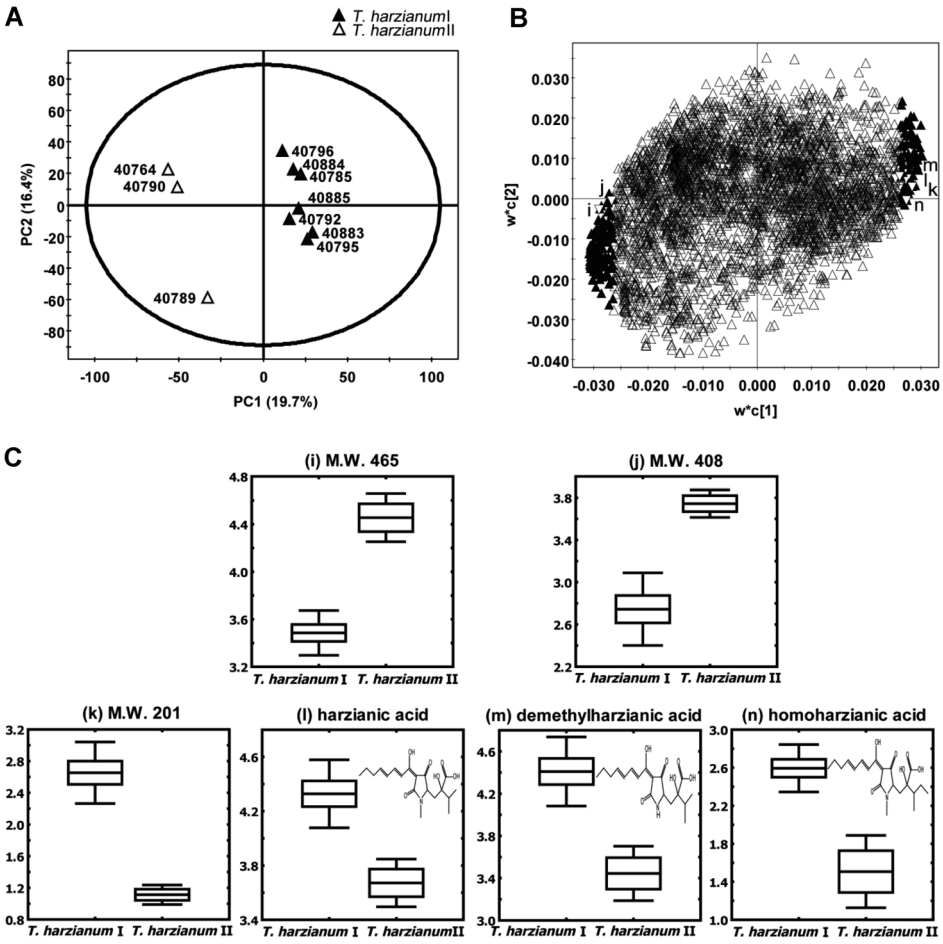

Fig. 5. PLS-DA score plots (**A**) and loading plots (**B**) of different clusters in the LC–MS-based dendrogram.
The selected variables (▲, VIP>2.0) and significantly different metabolites (▽) are highlighted in loading plots. Box-and-whisker plots showed significantly different secondary metabolites between *T. harzianum* I and II (**C**) (p<0.001). The Y axis of box-and-whisker plots indicates the LC–MS data transferred by $\log_{10}$.

ITS sequences and identification of secondary metabolites could provide a more accurate approach for *Trichoderma* classification.

T. harzianum strains were divided differently in the ITS-based phylogenetic tree (three subclusters) and secondary metabolite-based chemotaxonomy (two subclusters). In

Table 4. Significantly different metabolites between *T. koningii* and *T. atroviride.*

	LC–ESI–MS–MS				UPLC–Q-TOF		
Tentative identification	t_R (min)	MW	$[M-H]^-$ MS^n fragment ions (m/z)	p Value (t-test)[a]	Measured $[M-H]^-$	Error (ppm)	Ref.
N.I.	10.0	296	295, 277, 253, 183	4.50E-05	295.1497	-	-
N.I.	13.4	294	293, 275, 247, 231	5.90E-04	293.1397	-	-
N.I.	13.5	308	307, 263, 233, 205	1.30E-05	307.0829	-	-
N.I.	13.7	272	271, 253, 195, 183	8.68E-04	271.1899	-	-
N.I.	14.5	444	443, 329, 219, 281	4.86E-04	443.2231	-	-
Koninginin B or E	15.2	282	281, 219, 149, 123	4.26E-04	281.1745	2.5	[19]
Koninginin D	16.5	298	297, 279, 165, 149	8.00E-05	297.1699	0.7	[7]
N.I.	18.3	449	448, 404. 386, 371	6.10E-04	448.3022	-	-

t_R, Retention time; N.I., not identified.
[a]Indicated significant difference by t-test.

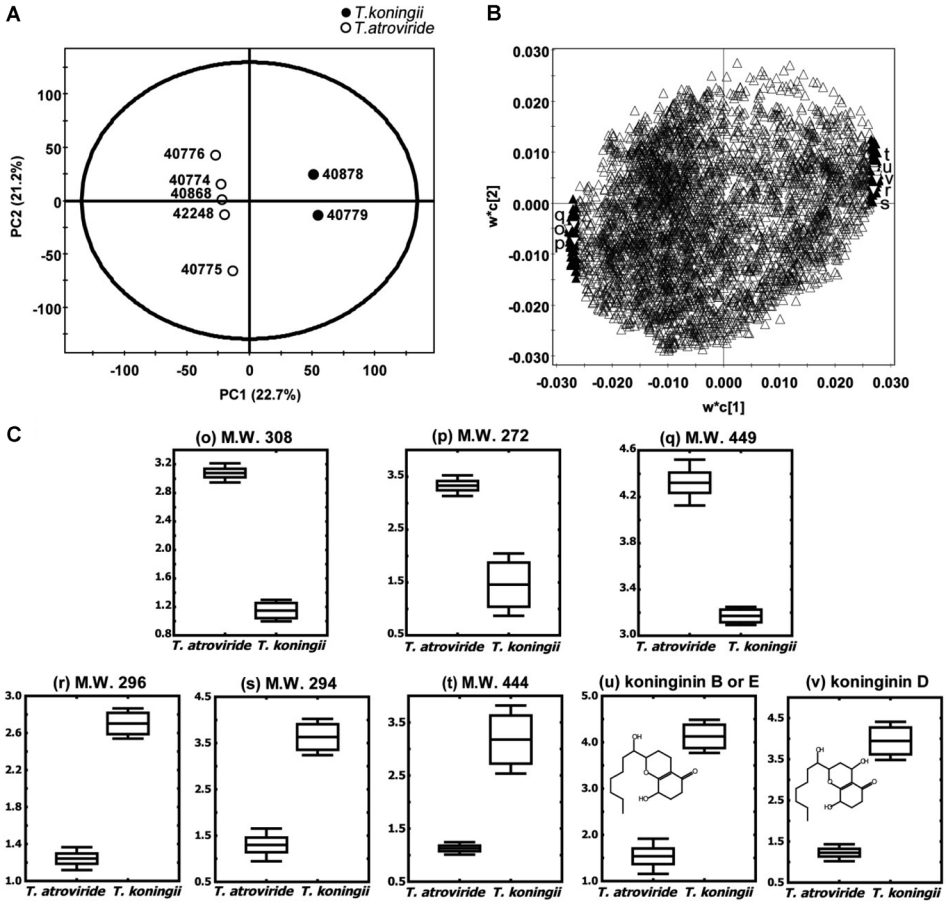

Fig. 6. PLS-DA score plots (**A**) and loading plots (**B**) of different clusters in the LC–MS-based dendrogram.
The selected variables (▲, VIP>2.0) and significantly different metabolites (▽) are highlighted in loading plots. Box-and-whisker plots showed significantly different secondary metabolites between *T. koningii* and *T. atroviride* (**C**) (p<0.01). The Y axis of box-and-whisker plots indicates the LC–MS data transferred by $\log_{10}$.

addition, *T. koningii* strains were mixed together with *T. atroviride* strains by the former approach; however, they formed an independent subcluster in the chemotaxonomic dendrogram. These observations suggest that ITS-based taxonomy alone may not be suitable for the elucidation of metabolic variations among species. Secondary metabolites are directly related to function. Ten secondary metabolites whose activities have been characterized in previous studies were identified in this study. *T. longibrachiatum* is known to produce sorbillin-related polyketides (*e.g.*, sorbicillinol, trichodermanone C, and bisorbicillinol), which have DPPH radical scavenging activity [2]. *T. koningii* produces koninginin D as the major metabolite, which has antifungal activity against plant pathogens such as *Rhizoctonia solani* and *Fusarium oxysporum* [10]. Harzianic acid is known to be a plant growth-promoting metabolite [28]. Secondary metabolite-based chemotaxonomy seems to be a more relevant approach to classifying *Trichoderma* species and understanding their potential uses.

In this study, *Trichoderma* species were categorized according to their secondary metabolite profiles obtained by LC–ESI–MS–MS, and this method seems to be an effective approach for classification. Tandem mass spectrometry analysis may be able to tentatively identify metabolites owing to their characteristic fragmentation patterns without the need for standard compounds; thus, this approach could perform the analysis simply and reliably using only small amounts of extracts. The identification of significantly different metabolites that were noted in previous studies demonstrates that LC–MS-based high-throughput multivariate statistical analysis adequately determined the characteristic metabolites of *Trichoderma* species.

The secondary metabolite-based chemotaxonomic technique is an important tool for identifying and classifying *Trichoderma* fungi according to species-specific metabolites. In addition, this metabolomic approach holds promise for the screening of non-targeted metabolites and may be an effective tool for selecting new functional metabolites from among species groups that represent diverse metabolite profiles. Finally, such an approach may provide new and important information on fungal metabolites that cannot be obtained using ITS-based taxonomy.

Acknowledgments

This work was supported by the Korea Science and Engineering Foundation (No. R01-2007-000-20231-0) and the Microbial Genomics and Application Center funded by the Korean Government (MEST), and partially by the Priority Research Centers Program through the National Research Foundation (NRF), Republic of Korea.

REFERENCES

1. Abe, N., T. Murata, and A. Hirota. 1998. Novel DPPH radical scavengers, bisorbicillinol and demethyltrichodimerol. *Biosci. Biotechnol. Biochem.* **62:** 661–666.
2. Abe, N., O. Sugimoto, K. I. Tanji, and A. Hirota. 2001. Sorbicillinol, a key intermediate of bisorbicillinoid biosynthesis in *Trichoderma* sp. USF-2690. *Biosci. Biotechnol. Biochem*. **65:** 2271–2279.
3. Abe, N., O. Sugimoto, K. I. Tanji, and A. Hirota. 2000. Identification of the quinol metabolite sorbicillinol, a key intermediate postulated in bisorbicillinoid biosynthesis. *J. Am. Chem. Soc*. **122:** 12606–12607.
4. Degenkolb, T., H. V. Dohren, N. F. Nielsen, G. J. Samuels, and H. Bruckner. 2008. Recent advances and future prospects in peptaibiotics, hydrophobin, and mycotoxin research, and their importance for chemotaxonomy of *Trichoderma* and *Hypocrea*. *Chem. Biodivers.* **5:** 671–680.
5. Druzhinina, I. S., A. G. Kopchinskiy, M. Komon, J. Bissett, G. Szakacs, and C. P. Kubicek. 2005. An oligonucleotide barcode for species identification in *Trichoderma* and *Hypocrea*. *Fungal Genet. Biol.* **42:** 813–828.
6. Druzhinina, I. S., A. G. Kopchinskiy, and C. P. Kubicek. 2006. The first 100 *Trichoderma* species characterized by molecular data. *Mycoscience* **47:** 55–64.
7. Dunlop, R. W., A. Simon, and K. Sivasithamparam. 1989. An antibiotic from *Trichoderma koningii* active against soilborne plant pathogens. *J. Nat. Prod.* **52:** 67–74.
8. Frisvad, J. C., B. Andersen, and U. Thrane. 2008. The use of secondary metabolite profiling in chemotaxonomy of filamentous fungi. *Mycol. Res.* **112:** 231–240.
9. Hoyos-Carvajal, L., S. Orduz, and J. Bissett, 2009. Genetic and metabolic biodiversity of *Trichoderma* from Colombia and adjacent neotropic regions. *Fungal Genet. Biol.* **46:** 615–631.
10. Itoh, Y., K. Kodama, K. Furuya, S. Takahashi, T. Haneishi, Y. Takiguchi, and M. Arai. 1980. A new sesquiterpene antibiotic, heptelidic acid producing organisms, fermentation, isolation and characterization. *J. Antibiot.* **33:** 468–473.
11. Kawada, M., Y. Yoshimoto, H. Kumagai, T. Someno, I. Momose, N. Kawamura, K. Isshiki, and D. Ikeda. 2004. PP2A inhibitors harzianic acid and related compounds produced by fungus strain F-1531. *J. Antibiot.* **57:** 235–237.
12. Kim, J., J. N. Choi, P. Kim, D. E. Sok, S. W. Nam, and C. H. Lee. 2009. LC–MS/MS profiling-based secondary metabolite screening of *Myxococcus xanthus*. *J. Microbiol. Biotechnol.* **19:** 51–54.
13. Kubicek, C. P., J. Bissett, I. Druzhinina, C. Kulling-Grandinger, and G. Szakacs. 2003. Genetic and metabolic diversity of *Trichoderma*: A case study on South-East Asian isolates. *Fungal Genet. Biol.* **38:** 310–319.
14. Kullnig, C. M., T. Krupica, S. L. Woo, R. L. Mach, M. Rey, T. Benifez, M. Lorito, and C. P. Kubicek. 2001. Confusion abounds over identities of *Trichoderma* of biocontrol isolates. *Mycol. Res.* **105**: 769–772.
15. Lommen, A. 2009. Metalign: Interface-driven, versatile metabolomics tool for hyphenated full-scan mass spectrometry data preprocessing. *Anal. Chem.* **81:** 3079–3086.
16. Lubeck, M., S. Bulat, I. Alekhina, and E. Lieckfeldt. 2004. Delineation of species within the *Trichoderma viride*/*atroviride*/*koningii* complex by UP–PCR cross-blot hybridizaion. *FEMS Microbiol. Lett.* **237:** 255–260.
17. Neumann, K., A. Abdel-Lateff, A. D. Wright, S. Kehraus, A. Krick, and G. M. Konig. 2007. Novel sorbicillin derivatives with an unprecedented carbon skeleton from the sponge-derived fungus *Trichoderma* species. *Eur. J. Org. Chem*. **14:** 2268–2275.
18. Nielsen, K. F., T. Grafenhan, D. Zarari, and U. Thrane. 2005. Trichothecene production by *Trichoderma brevicompactum*. *J. Agric. Food Chem.* **53:** 8190–8196.
19. Parker, S. R., H. G. Cutler, and P. R. Schreiner. 1995. Isolation of a biologically active natural product from *Trichoderma koningii*. *Biosci. Biotechnol. Biochem.* **59:** 1747–1749.
20. Pope, G. A., D. A. MacKenzie, M. Defernez, M. A. M. M. Aroso, L. J. Fuller, F. A. Mellon, *et al*. 2007. Metabolic footprinting as a tool for discriminating between brewing yeasts. *Yeast* **24:** 667–679.
21. Respinis, S. D., G. Vogel, C. Benagli, M. Tonolla, O. Petrini, and G. J. Samuels. 2010. MALDI–TOF MS of *Trichoderma*: Model system for the identification of microfungi. *Mycol. Progress* **9:** 79–100.
22. Singh, H. B. and D. P. Singh. 2009. From biological control to bioactive metabolites: Prospects with *Trichoderma* for safe human food. *J. Trop. Agric. Sci*. **32:** 99–110.
23. Smedsgaard, J. 1997. Micro-scale extraction procedure for standardized screening of fungal metabolite production in cultures. *J. Chromatogr. A* **760:** 264–270.
24. Tamura, K., J. Dudley, M. Nei, and S. Kumar. 2007. MEGA 4: Molecular evolutionary genetics analysis (MEGA) software version 4.0. *Mol. Biol. Evol.* **24:** 1596–1599.
25. Thrane, U., S. B. Poulsen, H. I. Nirenberg, and E. Lieckfeldt. 2001. Identification of *Trichoderma* strains by image analysis of HPLC chromatograms. *FEMS Microbiol. Lett.* **203:** 249–255.
26. Vinale, F., K. Sivasithamparam, E. L. Ghisalberti, R. Marra, M. J. Babetti, H. Li, S. L. Woo, and M. Lorito. 2008. A novel role for *Trichoderma* secondary metabolites in the interactions with plants. *Physiol. Mol. Plant Pathol*. **72:** 80–86.
27. Vinale, F., R. Marra, F. Scala, E. L. Ghisalberti, M. Lorito, and K. Sivasithamparam. 2006. Major secondary metabolites produced by two commercial *Trichoderma* strains active against different phytopathogens. *Lett. Appl. Microbiol*. **43:** 143–148.
28. Vinale, F., G. Flematti, K. Sivasithamparam, M. Lorito, R. Marra, B. W. Skelton, and E. L. Ghisaberti. 2009. Harzianic acid, an antifungal and plant growth promoting metabolite from *Trichoderma harzianum*. *J. Nat. Prod.* **72:** 2032–2035.